Inorganica Chimica Acta, 50 (1981) 71–80

Adducts of 1,4-Diazabutadienes with Group IIB Metal Halides

P. L. SANDRINI*, A. MANTOVANI

Cattedre di Chimica, Facoltà di Ingegneria, University of Padua, Padua, Italy

B. CROCIANI

Istituto di Chimica Generale, University of Palermo, Palermo, Italy

and P. UGUAGLIATI

Centro Chimica Tecnologia Composti Metallorganici Elementi Transizione C.N.R., Istituto di Chimica Industriale, Via Marzolo 9, Padua, Italy

Received January 8, 1981

The reactions of 1,4-diazabutadienes (or α-diimines) R–N=C(R')–C(R'')=N–R, DAB, (R = p-C_6H_4OMe, R' = R'' = H, DAB^I; R = p-C_6H_4OMe, R' = H, R'' = Me, DAB^{II}; R = p-C_6H_4OMe, R' = R'' = Me; DAB^{III}; R = CMe_3, R' = R'' = H, DAB^{IV}) with MX_2 (M = Zn, Cd, Hg; X = Cl, Br) yield in general 1/1 adducts. These species are assigned a monomeric configuration with a σ,σ'-N,N', chelating DAB ligand for M = Zn, Hg, whereas the $CdCl_2$ adducts have polymeric structures with terminal and/or bridging chlorides. In the reactions of $CdCl_2$ with DAB^I or DAB^{IV} polymeric species $[(CdCl_2)_2(DAB)]_x$ are obtained in which all chlorides are bridging. Spectrophotometric dissociation equilibrium constants have been determined by titration methods in 1,2-dichloroethane for some Zn and Hg 1/1 adducts. The stability constants depend markedly on the substituents on the imine C and N atoms. When R = CMe_3 (DAB^{IV}) no dissociation is detected, whereas with R = p-C_6H_4OMe the stability constants increase in the order: $DAB^I < DAB^{II} \leqslant DAB^{III}$ which is apparently the order of increasing σ-donor ability of the α-diimine ligands. The $[ZnCl_2(DAB^I)]$ complex is ca. 30 times more stable than its Hg analogue. Computational details of the equilibrium measurements are also discussed.

Introduction

In the past few years the chemistry of transition metal complexes with 1,4-diaza-1,3-butadienes (α-diimines), DAB, has received considerable attention in view of the versatile bonding capabilities of these ligands. In fact, besides the most common coordination mode, *i.e.* σ,σ'-N,N' chelating bidentate [1], they can also act as (i) either rigid σ-N or fluxional σ-N ↔ σ'-N' monodentate ligands [2], (ii) σ,σ'-N,N' bridging bidentate [3], (iii) σ-N, η^2-C=N' chelating bidentate [4]. Furthermore, in polynuclear complexes the DAB ligands may behave as six or eight electron donors through σ-N, σ'-N', η^2-C=N' [5] or σ-N, σ'-N', η^2-C=N, η^2-C=N' coordination types [6]. Several studies have been carried out on the σ-donor/π-acceptor properties of these ligands when acting as σ,σ'-N,N' chelating bidentate [1a, 7–9]. In general DAB ligands of the type R–N=C(R')–C(R')=N–R (R = alkyl or aryl group; R' = H, Me) have been found to be better π-acceptors than 2-pyridinealdehydeimines, 2,2'-bipyridine and 1,10-phenanthroline, in which the N=C–C=N skeleton is partly or totally incorporated into aromatic ring systems.

Recently, we have studied the preparation and coordination abilities of a series of organometallic palladium(II) complexes, wherein the metal is σ-bonded to a 1,4-diaza-1,3-butadiene-2-yl group [10]:

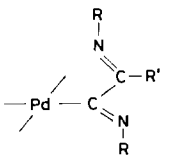

[R = p-C_6H_4X (X = H, Me, OMe), C_6H_{11}; R' = H, Me, Ph]

In general, the α-diimine moiety in these derivatives behaves as a σ,σ-N,N' chelating bidentate ligand towards a variety of transition metal ions. In the course of these lines of research the need has emerged for comparative investigations with the related 'purely organic' 1,4-diazabutadienes R–N=C(R')–

*Deceased.

C(R'')=N–R (R = *p*-C_6H_4OMe, CMe_3; R' = R'' = H, Me; R' = Me, R'' = H) [10e, 11]. We have now extended these studies to complexes of the latter ligands with group II B metal halides. These systems proved particularly suited for determining stability constants in the case of 1/1 DAB/HgX_2 adducts.

Experimental

The DAB^{I}, DAB^{III}, DAB^{IV} ligands were prepared and purified by the method of tom Dieck *et al.* [1a]. The preparation of DAB^{II} ligand is described elsewhere [11]. Anhydrous ZnX_2 and $CdCl_2$ halides were obtained by standard methods [12]. Solvents were dried and distilled before use.

[ZnX_2(DAB)] (X = Cl, Br)

A solution of anhydrous ZnX_2 (1 mmol) in *ca.* 50 ml of ethanol was treated with a solution of DAB (1.1 mmol) in *ca.* 15 ml of CH_2Cl_2. An immediate precipitation of the products occurred in all cases but with DAB^{IV}. The solvent mixture was partially evaporated at reduced pressure and the precipitation was completed by addition of ethyl ether. The precipitates consisted of [ZnX_2(DAB)] adducts in a virtually pure state and required no further purification.

With DAB^{IV}, the clear reaction mixture was concentrated to a small volume, whereupon the white [$ZnX_2(DAB^{IV})$] microcrystals began to separate. Complete precipitation was achieved by addition of an ethyl ether/n-hexane (2/1 v/v) mixture. The yields, based on ZnX_2, are in the range 55–85% (Molecular weight in 1,2-dichloroethane at 37 °C for [$ZnCl_2$-(DAB^{IV})]: Calcd. 304.5; Found 316).

[$CdCl_2$(DAB)]$_x$ (DAB = DAB^{II}, DAB^{III})

A solution of anhydrous $CdCl_2$ (1 mmol) in *ca.* 50 ml of hot ethanol was treated with a solution of DAB (1.1 mmol) in *ca.* 15 ml of CH_2Cl_2. The yellow [$CdCl_2(DAB^{II})]_x$ precipitated almost immediately, whereas the gold-yellow [$CdCl_2(DAB^{III})]_x$ began to precipitate after 10 min. The reaction mixture was stirred for 2 h, after which the solvents were partially evaporated at reduced pressure. The insoluble products were filtered off, washed with ethanol and dried *in vacuo*. Their insolubility prevented any further purification (yields: 75–85%).

[($CdCl_2$)$_2$(DAB)]$_x$ (DAB = DAB^{I}, DAB^{IV})

The reactions were carried out as described above for DAB^{II} and DAB^{III}. The resulting insoluble products were filtered off, washed with ethanol (and also with CH_2Cl_2 for the DAB^{I} derivative, in order to eliminate any trace of free ligand) and dried *in vacuo* (yields based on $CdCl_2$: 70–80%).

[HgX_2(DAB)] (X = Cl, Br)

These compounds were prepared by a procedure analogous to that of the corresponding ZnX_2 adducts. Owing to their moderate solubility in CH_2Cl_2, the products isolated from the reaction mixture (which in most cases were already satisfactorily pure) could be recrystallized from CH_2Cl_2/ethyl ether. In the case of the more soluble [$HgX_2(DAB^{IV})$], an ethyl ether/n-hexane (2/1 v/v) mixture was added to the CH_2Cl_2 solution. The yields are in the range 67–82%. (Molecular weight in 1,2-dichloroethane at 37 °C for [$HgCl_2(DAB^{IV})$]: Calcd. 440; Found 446).

Physical Measurements

Microanalyses were performed by A. Berton and G. Biasioli of the Microanalytical Laboratory, Laboratorio Radioelementi C.N.R., Padua. Molecular weights were determined using a Knauer osmometer. ^1H NMR spectra were recorded on a Varian EM-390 90 MHz spectrometer with tetramethylsilane (TMS) as internal standard. Electronic spectra in solution were recorded with a Bausch-Lomb Spectronic 210 spectrophotometer in the range 650–250 nm, using quartz cells of 1 cm path length. Infrared spectra were recorded with Perkin-Elmer 597 (4000–250 cm^{-1}) and Beckmann IR 11 (400–120 cm^{-1}) instruments, using hexachlorobutadiene mulls and NaCl plates in the range 4000–1300 cm^{-1}, Nujol mulls and either CsI (1700–250 cm^{-1}) or thin polythene discs (400–120 cm^{-1}).

Equilibrium Measurements

Equilibrium dissociation constants for MX_2–DAB 1/1 adducts were determined spectrophotometrically by recording the absorbances at various wavelengths in the range 500–300 nm of 1,2-dichloroethane solutions of MX_2 and DAB in various concentration ratios, such that the total concentration of DAB was maintained constant throughout (5×10^{-5} *M*). The solutions were made up by mixing appropriate volumes of standard solutions of the reactants and transferring them into the sample cell of the spectrophotometer in a thermostatted (±0.1 °C) compartment. The temperature was maintained constant by a water circulating Haake F-3C thermostat. The blank cell always contained the pure solvent since MX_2 does not absorb in the wavelength range examined. The statistical handling of absorbance data was carried out on a Tektronix 4052 Graphic System with 64K RAM memory equipped with a Tektronix 4662 Digital Plotter.

Results and Discussion

The reactions of group II B metal halides, MX_2 (M = Zn, Cd, Hg; X = Cl, Br) with 1,4-diaza-1,3-butadiene ligands R–N=C(R')–C(R'')=N–R, DAB

TABLE I. Analytical and Physical Data.

Compound	Colour	M.P. (°C)[a]	C[b]	H	N	Halide
$[ZnCl_2(DAB^I)]$	Yellow-orange	291	46.9 (47.50)	4.1 (3.99)	6.7 (6.92)	17.7 (17.52)
$[ZnBr_2(DAB^I)]$	Orange	283	38.9 (39.07)	3.6 (3.28)	5.8 (5.70)	32.2 (32.16)
$[(CdCl_2)_2(DAB^I)]_x$	Orange-red	>300	30.4 (30.26)	2.6 (2.54)	4.3 (4.40)	22.2 (22.33)
$[HgCl_2(DAB^I)]$	Brick-red	131	35.7 (35.60)	2.9 (2.98)	5.3 (5.19)	12.5 (13.13)
$[HgBr_2(DAB^I)]$	Orange	117	30.7 (30.65)	2.9 (2.57)	4.3 (4.45)	25.7 (25.22)
$[ZnCl_2(DAB^{II})]$	Yellow	201	48.8 (48.78)	4.6 (4.33)	6.7 (6.69)	16.8 (16.94)
$[ZnBr_2(DAB^{II})]$	Yellow	219	40.0 (40.36)	3.4 (3.57)	5.3 (5.52)	31.1 (31.27)
$[CdCl_2(DAB^{II})]_x$	Yellow	184	43.6 (43.85)	4.1 (3.90)	6.1 (6.02)	15.2 (15.23)
$[HgCl_2(DAB^{II})]$	Buff	97	36.6 (36.87)	3.5 (3.28)	5.4 (5.06)	11.9 (12.80)
$[ZnCl_2(DAB^{III})]$	Yellow	296	50.3 (49.96)	4.7 (4.66)	6.3 (6.47)	16.8 (16.38)
$[ZnBr_2(DAB^{III})]$	Yellow	>300	41.8 (41.58)	4.1 (3.89)	5.3 (5.39)	30.6 (30.42)
$[CdCl_2(DAB^{III})]_x$	Gold-yellow	206	45.4 (45.06)	4.1 (4.20)	5.9 (5.84)	15.2 (14.78)
$[HgCl_2(DAB^{III})]$	Yellowish	132	37.5 (38.07)	3.5 (3.55)	4.8 (4.93)	12.5 (12.48)
$[HgBr_2(DAB^{III})]$	Yellow	151	33.1 (33.00)	3.0 (3.07)	4.2 (4.26)	24.3 (24.14)
$[ZnCl_2(DAB^{IV})]$	White	285	39.6 (39.44)	6.6 (6.62)	9.1 (9.20)	23.1 (23.28)
$[ZnBr_2(DAB^{IV})]$	White	268	30.4 (30.65)	4.9 (5.14)	7.1 (7.15)	40.4 (40.37)
$[(CdCl_2)_2(DAB^{IV})]_x$	White	>300	22.4 (22.45)	3.9 (3.77)	5.2 (5.24)	26.5 (26.51)
$[HgCl_2(DAB^{IV})]$	White	177	26.4 (27.31)	4.5 (4.58)	6.1 (6.37)	15.6 (16.12)
$[HgBr_2(DAB^{IV})]$	White	176	21.0 (22.79)	3.7 (3.81)	5.2 (5.30)	30.1 (30.01)

[a] Uncorrected values: all compounds decompose on melting. [b] Calcd. values in parenthesis.

(R = *p*-C_6H_4OMe, R′ = R″ = H, DAB^I; R = *p*-C_6H_4OMe, R′ = H, R″ = Me, DAB^{II}; R = *p*-C_6H_4OMe, R′ = R″ = Me, DAB^{III}; R = CMe_3, R′ = R″ = H, DAB^{IV}) in a 1/1 molar ratio proceed as follows. All the $CdCl_2$ adducts are insoluble polymeric compounds (see further) with a Cd/DAB ratio of 1/1 or 2/1, depending on the imino-carbon substituents R′, R″. The latter ratio occurs only with R′ = R″ = H, whatever the imino-nitrogen substituents. Analytical and physical data are listed in Table I whereas

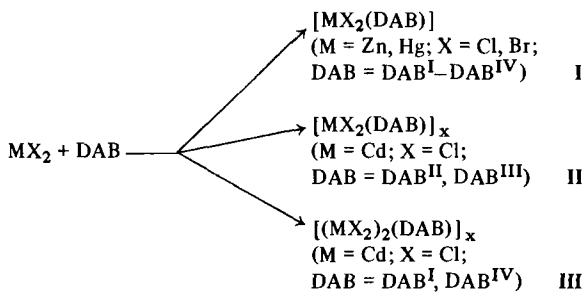

TABLE II. Selected IR and ^{1}H NMR Spectroscopic Data.

Compound	IR Absorptions[a]		^{1}H NMR Signals[b]				
	ν(C=N)	ν(M–X)	N=C–H	$-C_6H_4-$	O–Me	C–Me	CMe_3
DAB^I	1609s; 1605sh; 1584ms; 1580sh		8.35 S	7.4–6.8 M[c]	3.77 S		
$[ZnCl_2(DAB^I)]$	1622mw; 1586s	335m; 321m					
$[ZnBr_2(DAB^I)]$	1622mw; 1586s	279m; 256m					
$[(CdCl_2)_2(DAB^I)]_x$	1621s; 1590s	200m, br					
$[HgCl_2(DAB^I)]$	1631w; 1590s	286m; 257m, br	8.44 S	7.4–6.8 M[c]	3.80 S		
$[HgBr_2(DAB^I)]$	1631w; 1588s	197m; 189m	8.47 S	7.5–6.8 M[c]	3.84 S		
DAB^{II}	1615s; 1600s; 1583ms; 1578ms		8.15 S	7.4–6.6 M[c]	3.72 S	2.15 S	
$[ZnCl_2(DAB^{II})]$	1646w; 1548w	340ms; 321m					
$[ZnBr_2(DAB^{II})]$	1648mw; 1556mw	250ms					
$[CdCl_2(DAB^{II})]_x$	1649m; 1552ms	270m; 230m, br					
$[HgCl_2(DAB^{II})]$	1639w; 1534mw	300ms; 260m	8.45 S	7.6–6.6 M[c]	3.79 S	2.36 S	
DAB^{III}	1632s; 1604s; 1578w			6.9–6.6 M[c]	3.75 S	2.10 S	
$[ZnCl_2(DAB^{III})]$	1650m; 1609s; 1590m; 1580m	331s; 314s					
$[ZnBr_2(DAB^{III})]$	1650mw; 1609s 1589m; 1581m	256sh; 251ms					
$[CdCl_2(DAB^{III})]_x$	1658m; 1609s; 1586m	273m, 218m, br					
$[HgCl_2(DAB^{III})]$	1668m; 1609s; 1580m	274s; 255sh		6.87 S	3.75 S	2.22 S	
$[HgBr_2(DAB^{III})]$	1666mw; 1610s; 1580m	191m, s; 185m		6.92 S	3.79 S	2.28 S	
DAB^{IV}	1630s		7.93 S				1.29 S
$[ZnCl_2(DAB^{IV})]$	1660w; 1596mw	333s; 321s	8.29 S				1.50 S
$[ZnBr_2(DAB^{IV})]$	1660mw; 1597m	260s; 250sh	8.29 S				1.54 S
$[(CdCl_2)_2(DAB^{IV})]_x$	1674mw; 1618m	210m, br					
$[HgCl_2(DAB^{IV})]$	1675m; 1610m	270s; 255sh					
$[HgBr_2(DAB^{IV})]$	1674m; 1609m	190sh; 186m	8.32 S				1.45 S

[a]The assignment of ν(C=N) bands for the ligands with R = *p*-C_6H_4OMe is complicated by the occurrence of intense absorptions of the *para*-substituted phenyl groups around 1600 and 1500 cm^{-1}. [b]Spectra recorded in $CDCl_3$ at 35 °C; δ values in ppm from TMS as internal standard; S = singlet, M = multiplet. [c]AA'BB' symmetrical multiplet.

selected IR and ^{1}H NMR spectral data are shown in Table II. Molecular weight measurements together with IR, ^{1}H NMR and electronic spectral features suggest a monomeric pseudo-tetrahedral configuration for adducts **I**. The solubility of these compounds is markedly influenced by the imino-nitrogen R substituents of DAB and, to a lesser extent, by the central metal M. When R = CMe_3, soluble products are obtained for both ZnX_2 and HgX_2 derivatives, the molecular weights of which in 1,2-dichloroethane at 37 °C are in good agreement with the theoretical values for monomeric undissociated $[MX_2(DAB^{IV})]$ compounds (see Experimental). Their ^{1}H NMR spectra are characterized by one sharp singlet at δ *ca.* 8.3 ppm (N=C–H) and by one sharp singlet at δ *ca.* 1.5 ppm (CMe_3) with a relative intensity of 1/9, both signals being down-field shifted compared to free DAB^{IV}. All these features point to a symmetrical σ,σ'-N,N' chelating bidentate coordination mode [2, 3a, 4b, 11, 13]. When R = *p*-C_6H_4OMe, the mercury derivatives $[HgX_2(DAB)]$ (DAB = DAB^I, DAB^{II}, DAB^{III}) are moderately soluble in halogenated

solvents, which enabled molecular weight measurements and ^{1}H NMR spectra recording.

M.W. and electronic spectral data showed that dissociation takes place upon dilution, to an extent which depends on the nature of DAB (see further). The ^{1}H NMR spectra of $CDCl_3$ saturated solutions are again consistent with σ, σ'-N,N' chelating bidentate DAB ligands [δ(N=C–H) and δ(C–Me) signals shifted 0.1–0.3 and 0.1–0.2 ppm down-field respectively from the free ligands].

The low solubility of the zinc analogs, [ZnX_2-(DAB)] (DAB = DAB^{I}, DAB^{II}, DAB^{III}) prevented any physical measurements in solution other than electronic spectra. However, these compounds are also likely to have the same configuration as the soluble [ZnX_2(DAB^{IV})] derivatives on account of the following observations.

i) Zn–X stretching frequencies are very close to those reported for pseudo-tetrahedral mononuclear complexes [ZnX_2L_2] (L = N-donor ligand) [14], and for binuclear 1,4-diazabutadiene derivatives of type **IV** [10b, d, f]:

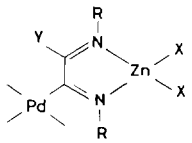

(IV)

(R = *p*-C_6H_4OMe; X = Cl, Br; Y = H, Me)

therefore, no halide-bridges are present in the solid.

ii) The electronic spectra of [ZnX_2(DAB)] in 1,2-dichloroethane solution match those of **IV** in the range 350–550 nm, where typical Zn → 1,4-diazabutadiene CT bands occur [15] (Fig. 1), implying that the same 5-membered metallocyclic chromophore is present in both series of compounds.

Apparently, the solubility of ZnX_2–1,4-diazabutadiene adducts is governed by the steric requirements of both N- and C-imino substituents, probably in connection with solid state packing effects. Replacing the *p*-C_6H_4OMe N-substituents with the bulkier CMe_3 groups brings about a marked increase in solubility for DAB^{IV} derivatives. An analogous effect is observed when replacing a proton or methyl C-substituent with a σ-bonded square planar palladium moiety in **IV**.

The number and position of ν(Hg–X) bands in the HgX_2 adducts are also consistent with a pseudo-tetrahedral arrangement (with terminal halides) being present in the solid state [14a, 16].

The cadmium derivatives **II** display two quite distinct Cd–Cl stretching vibrations, *ca.* 40–50 cm^{-1} apart. Whereas the higher frequency band (about 270 cm^{-1}) can be confidently assigned to terminal Cd–Cl bands, the lower frequency one is better interpreted in terms of bridging chlorides [17]. Therefore a

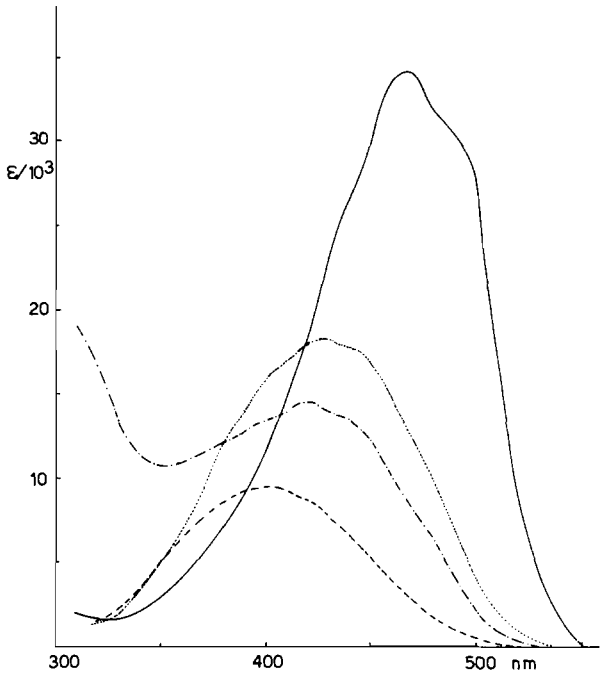

Fig. 1. Electronic spectra (300–550 nm) in 1,2-dichloroethane at 25 °C of [$ZnCl_2$(DAB^{I})] (———); [$ZnCl_2$(DAB^{II})] (·····); [$ZnCl_2$(DAB^{III})] (— — —) and the 1/1 adduct between *trans*-[PdCl{C(=NR)CH=NR}(PPh_3)$_2$] (R = *p*-C_6H_4OMe) and $ZnCl_2$ (• — • — •).

polymeric chloride-bridged structure in which the Cd atom achieves a coordination number higher than four is involved in the solid state, consistent with the low solubility of these compounds.

A very close far IR spectrum is also shown by the binuclear complex [10d]:

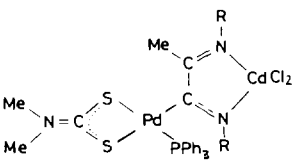

[ν(Cd–Cl) = 273ms, 217m]

However, in this case the chloride bridges are easily broken in solution thanks to the steric and lyophilic properties of the Pd(dmtc)PPh_3 imino-carbon substituent.

In the case of $CdCl_2$–DAB^{I} and –DAB^{IV} derivatives (**III**), only bridging chlorides are present in the solid state as indicated by the occurrence of one rather broad ν(Cd–Cl) band of medium intensity at 200–210 cm^{-1}. Similar far IR spectra were observed for complexes [$CdCl_2$(N–N)] [N–N = 2,2'-bipyridine and 1,10-phenanthroline; ν(Cd–Cl) at *ca.* 220 cm^{-1}] for which polymeric distorted octahedral

configurations were inferred [14a]. Although the insolubility of **III** prevents any characterization in solution, the $CdCl_2$/DAB 2/1 stoichiometric ratio raises some suspicion about the 1,4-diazabutadienes also acting as bidentate bridging ligands [3].

The ν(C=N) bands of free and coordinated 1,4-diazabutadienes are easily assigned for DAB^{IV} (R = CMe_3) whereas for DAB^{I}, DAB^{II} and DAB^{III} (R = *p*-C_6H_4OMe) this assignment is hampered by the presence of strong absorptions of the *p*-C_6H_4OMe group around 1600 and 1500 cm^{-1}. A typical feature of all spectra is a weak-to-medium band in the range 1621–1675 cm^{-1}, which might be either a combination or an overtone, or the symmetrical C=N stretch. We favour the latter assignment since this band is present in all the adducts and appears to depend on both DAB and central metal. Two ν(C=N) vibrations at much lower frequencies have been observed in the complexes [CuI(DAB^{IV})] [15] and [$M(CO)_4$·(DAB^{IV})] (M = Cr, Mo, W) [1c], in which an extensive π-back-donation of *d* electrons from the metal to the anti-bonding orbitals of DAB^{IV} takes place. Apart from differences in coordination numbers and structures, the higher values of ν(C=N) in the pseudo-tetrahedral compounds [$MX_2(DAB^{IV})$] (M = Zn, Hg) can be essentially ascribed to a scarce contribution of π back-bonding in these formally M^{2+} derivatives.

Dissociation Equilibrium Studies

The system

$$HgX_2 + DAB \rightleftarrows [HgX_2(DAB)] \quad (1)$$

was investigated in 1,2-dichloroethane in the temperature range 20–40 °C (X = Cl; DAB = DAB^{I}, DAB^{II}, DAB^{III}) or at 25 °C (X = Br; DAB = DAB^{I}) by spectrophotometric titration of DAB (*ca.* 5×10^{-5} *M*) with HgX_2, which does not absorb in the wavelength range examined (520–340 nm). Successive aliquots of a standard solution of HgX_2 were added to a solution of DAB in such a way that the total analytical concentration of the latter was kept constant throughout, and the UV–visible absorption spectra of the resulting solutions were recorded. A sharply defined isosbestic point was observed at *ca.* 400 nm, suggesting that only two species were absorbing independently in the vicinity of this wavelength, namely DAB and the adduct [HgX_2(DAB)]. Since the number of absorbing species would dictate the choice of the nonlinear regression model to be used in the subsequent data handling process, we confirmed such number to be 2 throughout the spectral region by means of Abstract Factor Analysis, a minicomputer implementation of which has recently been performed by one of us (P.U.) [18a]. A brief outline of the method is described in the following section.

Abstract factor analysis of absorbance data

The absorbance data of G solutions at N wavelengths (typically, G = 4–6, N = 10–15) are first organized into a data matrix **P** which according to Lambert–Beer's law can be expressed as:

$$\mathbf{P} = \mathbf{EC}$$

where **E** is the matrix of extinction coefficients of the components (unit path length cells) and **C** is the matrix of their molar concentrations in the mixture. The correct dimensions of the resulting data space (*factors*) are determined by a complete eigenanalysis of the dispersion matrix,

$$\mathbf{A} = \mathbf{P}^T\mathbf{P} \quad (N > G)$$
$$\mathbf{A} = \mathbf{P}\mathbf{P}^T \quad (N \leqslant G)$$

Since the data matrix **P** contains experimental error to some level, the rank of **A** is min(N, G), whereas the number of absorbing species (*factors*) is an upper bound to the ranks of either **E** or **C**. As a consequence, matrix **A** will have as many as N (or G, whichever is smaller) non-zero eigenvalues due to experimental error and the correct number of species can only be deduced with a fair degree of confidence by a combination of criteria. Our algorithm uses the following factor selection criteria:

i) Relative size of sorted eigenvalues of A: the relative magnitude of an eigenvalue is a measure of the relative contribution of the corresponding eigenvector to the variance of the data (*i.e.*, the more important factors correspond to the larger eigenvalues).

ii) Use of Malinowski's Real Error (RE) and Indicator (IND) Functions. Malinowski [18b, 19] has shown that the eigenvalues of A can be grouped into a primary set which contains the true factors and a secondary set consisting of pure error. A criterion for deducing the number of primary eigenvalues is provided by his Real Error Function, which approaches the estimated experimental error when all true factors have been included in its computation. Another criterion is provided by the number of factors at which the empirical function IND = RE/$(h-p)^2$ minimizes, where h = min(N, G), p = suspected number of factors. Its use also allows an assessment of the experimental error in the data set as the value of RE corresponding to that p which minimizes IND.

iii) Minimum number of eigenvectors needed to reproduce the original data set within a predefined error level. The original data matrix **P** is reconstructed by using the transforms $\mathbf{P}^* = \mathbf{P}\mathbf{B}(p)\mathbf{B}^T(p)$ (N > G) or $\mathbf{P}^* = \mathbf{B}(p)\mathbf{B}^T(p)\mathbf{P}$ (N ⩽ G) where $\mathbf{B}(p)$ is the matrix of orthonormalized eigenvectors with the lowest $h-p$ eigenvectors zeroed out. The transforms are compared pointwise with **P** for every eigenvalue up to **p**. The number of factors is chosen as the highest **p**

for which $\mathbf{P}^*$ reproduces $\mathbf{P}$ within experimental error. In practice, two evaluators of goodness of fit are examined. The first is the Exner [20] function: close agreement between the reproduced and the original data set is indicated by an Exner value close to zero (this function undergoes usually a marked decrease in correspondence to the true number of factors, F). The second evaluator is the Estimated Standard Error in the reproduction (ESE), which is also a decreasing function of p with a break at $p \rightarrow F$. Close fit is again indicated by an ESE value approaching the experimental error level [18a, 21]:

$$ESE(p) = \left(\frac{\Sigma\Sigma R^2}{(N-p)(G-p)}\right)^{1/2}$$

$$EXNER(p) = \left(\frac{\Sigma\Sigma R^2}{\Sigma\Sigma \bar{R}^2} \cdot \frac{NG}{(NG-p)}\right)^{1/2}$$

where $R = P^*_{iJ} - P_{iJ}$ (reconstruction residual). Further, the distribution of standardized residuals $R' = (P^*_{iJ} - P_{iJ})/S_0$ (S_0 = suspected level of experimental error) is computed by tallying their incidences in the variance ranges $0–S_0$, $S_0–2S_0$, $2S_0–3S_0$ *etc.*, and the chi square statistics $CHI = \Sigma\Sigma R'^2$ compared with the expectation value $(N-p)(G-p)$: if S_0 is close to the true experimental error then CHI tends to the latter for $p \rightarrow F$ [22]. As an additional aid in the choice of F, it can be shown that when the correct number of factors is reached, the residuals will virtually reproduce the noise level of the data, *i.e.*, they will be randomly (normally) distributed with zero mean and standard deviation close to the experimental error [18a].

The results of abstract factor analysis of absorbance data by means of the above described computer program are shown in Table III for the $HgCl_2/DAB^I$ system at 35 °C. In this Table are listed the eigenvalues, RE and IND values from eigenanalysis of a 15 X 4 absorbance matrix *versus* the suspected possible number of factors p. As can be seen, there is a sudden drop in both the eigenvalues and RE when $p > 2$, indicating that two factors are needed to span the data space; the first two eigenvalues account for 99.9998% of the total variance of the data. The IND function minimizes at $p = 2$. The corresponding RE value indicates that the experimental error in the data is close to 0.0011 absorbance unit. Table III also lists the results of reconstruction of the original data matrix with up to three eigenvectors within an experimental error of 0.0011 absorbance unit.

The distribution of standardized residuals also shows that two factors are required to reproduce the original data set within the noise level of the data, since CHI(0.0011, 2) is closest to the expectation statistics for $p = 2$ [26]. The estimated standard error for the 2-eigenvector reproduction, ESE(2), is almost identical to 0.0011 and the Exner function settles down to 0.003 for $p = 2$.

TABLE III. Results of Abstract Factor Analysis of a 15 X 4 Absorbance Matrix for the System $HgCl_2/DAB^I$ in DCE, 35 °C.

1) *Eigenanalysis*

No. of Factors	Eigenvalues	RE	IND
1	18.29	0.1266	0.0141
2	0.72	0.0011	2.695E – 4
3	2.14E – 5	0.0009	9.486E – 4
4	1.35E – 5	Undefined	Undefined

2) *Reconstruction*

Tallied Frequencies of Normalized Residuals in the Variance Ranges (S_0 = 0.0011 absorbance unit)

No. of Factors	0–1	1–2	2–3	3+	CHI[a]	Expected CHI
1	0	0	0	60	537859	42
2	50	10	0	0	26	26
3	59	1	0	0	10	12

Reproduction Statistics

No. of Factors	EXNER	ESE
1	0.524	0.1310
2	0.003	0.0011
3	0.002	0.0011

[a] Rounded to smaller closest integer.

TABLE IV. Statistical Properties of Sample of Sixty Residuals from 2-Eigenvector Reconstruction of 15 X 4 Absorbance Matrix for the System $HgCl_2/DAB^I$ (DCE; 35 °C) by Abstract Factor Analysis.

NG	60
Total	–1.7E – 5
Mean	–2.8E – 7
Variance	5.9E – 7
Std. Dev.[a]	7.7E – 4
Min.	–0.0018
Max.	0.0018
Range	0.0037
Skewness	–0.11
Kurtosis	3.2
3rd Moment	–4.8E – 11
4th Moment	1.1E – 12
Coeff. of Var.	–2700.9

[a] Calculated as $(\Sigma\Sigma(R-\bar{R})^2/(NG-1))^{1/2}$; related to ESE by the eqn.: $ESE \cong (\text{Std. Dev.}) \cdot [(NG-1)/((N-2)(G-2))]^{1/2}$.

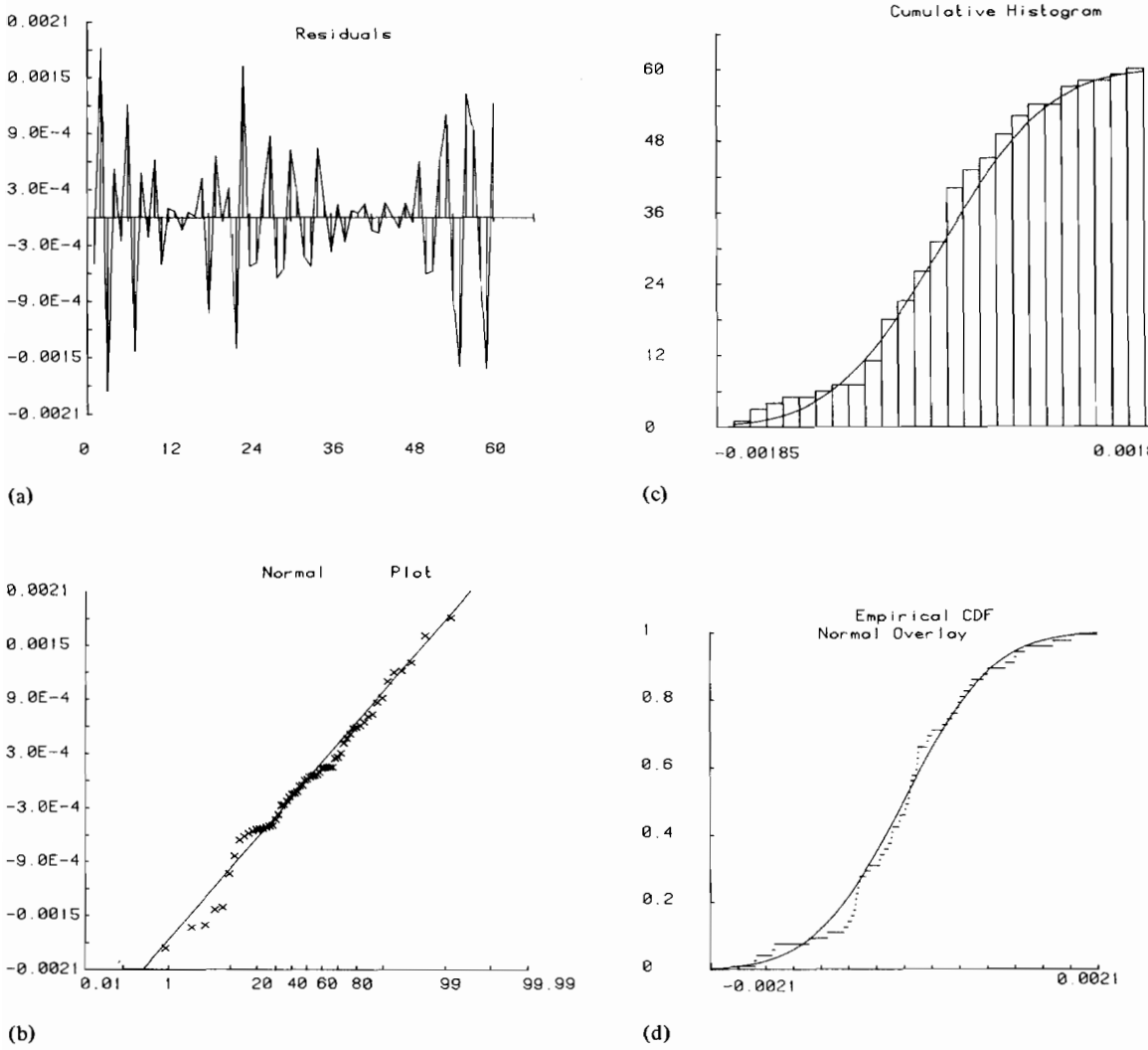

Fig. 2. One sample statistical analysis of residuals from 2-eigenvector reconstruction of original data matrix after Abstract Factor Analysis of a 15 × 4 absorbance data matrix for the system $HgCl_2/DAB^I$ at 35 °C. a) Residuals (vertical bars; successive residuals are connected by straightline segments); b) Normal Probability Plot; c) Cumulative Histogram; e) Empirical Cumulative Distribution Function with normal overlay.

The results of a thorough statistical analysis of the sample of sixty residuals after the 2-eigenvector reconstruction are presented in Table IV and in Figs. 2a–d [23]. As can be seen, the residuals are not highly patterned (Fig. 2a), have amplitudes within 2σ (0.002 absorbance unit), and appear to belong to a normal distribution* with zero mean and stand. dev. close to σ. Fig. 2b shows a normal probability plot of the residuals with the corresponding straight-line expected for normality [24], whereas Figs. 2c and 2d show the cumulative histogram and empirical cumulative distribution function with normal curve overlay, respectively [25].

*Compatibly with the rather small sample size being considered, of course.

The collective evidence gathered in this way unmistakably shows that in the system $HgCl_2/DAB^I$ under consideration there are only *two* independently absorbing species (DAB^I and $[HgCl_2(DAB^I)]$ in eqn. 1) which rules out the occurrence of possible metal–ligand interactions other than simple 1/1 adduct formation. The same conclusions were arrived at by abstract factor analysis of absorbance data for X = Br, DAB = DAB^{II}, DAB^{III}.

Determination of dissociation constants

Non-linear regression of absorbance data *vs.* the concentration of added HgX_2 for the system in eqn. 1 was carried out according to the following model [26].

Let M = HgX_2, L = DAB, ML = $[HgX_2(DAB)]$.

Then:

$[M][L]/[ML] = K_D$

$[ML] + [M] = a$ (*ca.* 5×10^{-5} *M*)

$[ML] + [L] = b$

$[ML] = \frac{1}{2}\{(a + b + K_D) - [(a + b + K_D)^2 - 4ab]^{1/2}\}$

$A_\lambda = \epsilon^\lambda_{ML}[ML] + \epsilon^\lambda_L[L]$

where a and b are the total analytical concentrations of M and L, respectively, A_λ is the absorbance at wavelength λ, ϵ^λ is the molar extinction coefficient at λ.

The function minimized was

$$\phi = \phi(\epsilon_i, K_D) = \Sigma (A_{obs} - A_{calcd})^2$$

with ϵ^λ_{ML} and K_D being the refined parameters. The values of ϵ^λ_L were previously determined from solutions of pure L. No weighting scheme was applied. The minimization was carried out by an optimized version of Marquardt's [27] algorithm implemented on the Tektronix 4052 (64K) Graphic System [28]. Good starting guesses for the parameter vector were obtained by a preliminary Nelder–Mead Simplex search [29].

At convergence, the parameter correlation matrix indicated that ϵ^λ_{ML} and K_D are fairly highly correlated, which resulted in the latter changing slightly with the wavelength. Therefore the non-linear fit was carried out for a series of wavelengths and the K_D values from individual fits were used to compute a weighted average value. It can be shown that this simplified procedure leads substantially to the same results as the more involved minimization of a multiresponse objective function [30]. Uncertainties quoted for K_D are averaged standard errors of estimate.

The dissociation constants at 25 °C in DCE are listed in Table V. Also included is the value for the system $ZnCl_2/DAB^I$ which was determined by the same procedure. Table VI lists the dependence of K_D for the system $HgCl_2/DAB^I$ on temperature in the range 20–40 °C. Non-linear regression of K_D *vs.* T according to the reparametrized model

$K_D = A \exp(-B/T^*)$

TABLE V. Dissociation Equilibrium Constants for the System $[MX_2(DAB)] \rightleftarrows MX_2 + DAB$ in DCE at 25 °C.

DAB = R–N=C(R')–C(R'')=N–R

R'	R''	M	X	$10^3 K_D, M$
H	H	Hg	Cl	2.41 ± 0.04
H	H	Hg	Br	1.60 ± 0.02
H	Me	Hg	Cl	0.7 ± 0.2
Me	Me	Hg	Cl	0.58 ± 0.03
H	H	Zn	Cl	0.07 ± 0.007

TABLE VI. Dependence of K_D on Temperature for the System $HgCl_2/DAB^I$ in DCE (uncertainties are standard errors of estimate).

Temp., °C	$10^3 K_D, M$	Thermodynamic Parameters
20	2.02 ± 0.03	ΔH^0 = 8.6 ± 0.6 Kcal/mol
25	2.41 ± 0.04	ΔS^0 = 17 ± 2 e.u.
30	3.6 ± 0.2	
35	4.07 ± 0.02	
40	4.5 ± 0.4	

(weighting scheme: $w_i = 1/\sigma_i^2$) gave the following values of thermodynamic parameters: ΔH^0 = 8.6 ± 0.6 Kcal/mol; ΔS^0 = 17 ± 2 e.u. The formulation of this model [in which $A = \exp(\Delta S^0/R - \Delta H^0/RT_0)$, $B = -\Delta H^0/R$, $1/T^* = 1/T_0 - 1/T$, T_0 = average absolute temperature] has been shown to be particularly efficient in reducing the correlation between the parameters and improving their estimate [31].

The high correlation between the extinction coefficient of the adduct and the dissociation constant referred to above is a typically unavoidable feature of equilibrium studies based on spectrophotometric data measurements [32], which stems from the very nature of the mathematical model underlying the data reduction process. A large correlation coefficient may lead to large uncertainties in the parameters even though the fit of observed to calculated data is quite satisfactory. Correlation coefficients are unfortunately independent of the accuracy of measured data and of the number of wavelengths at which measurements are made and little prospects for reducing them exist other than widening the range of concentrations of ligand (or metal, in our case) being explored.

As can be seen in Table V, the K_D values decrease with increasing substitution by the electron-donating methyl group in the diimine C–C chain, showing that the stability of 1/1 adducts increases in the order $DAB^I < DAB^{II} \leqslant DAB^{III}$, which is the order of increasing σ-donor ability of the diazabutadiene ligands, as expected. The greatest effect is observed on substitution of the first hydrogen atom. The stability also increases on replacing the metal chloride with bromide. A dramatic increase in stability is observed for the zinc adduct. Table VI shows that dissociation of the adduct $[HgCl_2(DAB^I)]$ is an endothermic process with a positive entropy change.

References

1 a) H. tom Dieck and I. W. Renk, *Chem. Ber., 104,* 110 (1971) and references therein. b) P. Krumholz, O. A. Serra and M. A. De Paoli, *Inorg. Chim. Acta, 15,* 25 (1975). c) L. H. Staal, D. J. Stufkens and A. Oskam, *Inorg. Chim. Acta, 26,* 255 (1978). d) R. W. Balk, D. J. Stufkens and A. Oskam, *Inorg. Chim. Acta, 28,* 133 (1978).

2 H. van der Poel, G. van Koten and K. Vrieze, *Inorg. Chem., 19,* 1145 (1980).
3 a) H. van der Poel, G. van Koten and K. Vrieze, *J. Organometal. Chem., 135,* C63 (1977). b) H. van der Poel, G. van Koten, K. Vrieze, M. Kokkes and C. H. Stam, *Inorg. Chim. Acta, 39,* 197 (1980).
4 a) D. Leibfritz and H. tom Dieck, *J. Organometal. Chem., 105,* 255 (1976). b) L. H. Staal, A. Oskam and K. Vrieze, *J. Organometal Chem., 145,* C7 (1978).
5) a) H. W. Frühauf, A. Landers, R. Goddard and C. Krüger, *Angew. Chem., 90,* 56 (1978). b) L. H. Staal, L. H. Polm, G. van Koten and K. Vrieze, *Inorg. Chim. Acta, 37,* L485 (1979).
6 L. H. Staal, L. H. Polm, K. Vrieze, F. Ploeger and C. H. Stam, *J. Organometal. Chem., 199,* C13 (1980).
7 H. tom Dieck, K. D. Franz and F. Hohmann, *Chem. Ber., 108,* 163 (1975).
8 a) J. Reinhold, R. Benedix, P. Birner and H. Hennig, *Z. Chem., 17,* 115 (1977). b) *Idem, Inorg. Chim. Acta, 33,* 209 (1979).
9 R. W. Balk, *Thesis,* University of Amsterdam (1980) and references therein.
10 a) B. Crociani, M. Nicolini and R. L. Richards, *J. Organometal. Chem., 104,* 259 (1976). b) *Idem, J. Chem. Soc. Dalton Trans.,* 1478 (1978). c) B. Crociani and R. L. Richards, *J. Organometal. Chem., 154,* 65 (1978). d) B. Crociani, M. Nicolini and A. Mantovani, *J. Organometal. Chem., 177,* 365 (1979). e) B. Crociani, U. Belluco and P. L. Sandrini, *J. Organometal. Chem., 177,* 385 (1979). f) P. L. Sandrini, A. Mantovani and B. Crociani, *J. Organometal. Chem., 185,* C13 (1980).
11 B. Crociani, T. Boschi and P. Uguagliati, *Inorg. Chim. Acta, 48,* 9 (1981).
12 A. R. Pray, *Inorg. Synth., 5,* 153 (1957).
13 H. tom Dieck and A. Orlopp, *Angew. Chem., Int. Ed., 14,* 251 (1975).
14 a) G. E. Coates and D. Ridley, *J. Chem. Soc.,* 166 (1964). b) R. J. H. Clark and C. S. Williams, *Inorg. Chem., 4,* 350 (1965).
15 H. tom Dieck and I. W. Renk, *Chem. Ber., 104,* 92 (1971).
16 G. B. Deacon, J. H. S. Green and D. J. Harrison, *Spectrochim. Acta, 24A,* 1921 (1968).
17 P. L. Goggin, R. J. Goodfellow and K. Kessler, *J. Chem. Soc. Dalton Trans.,* 1914 (1977).
18 a) P. Uguagliati, A. Benedetti, S. Enzo and L. Schiffini, submitted. b) For an excellent survey on the scope and applications of this branch of multivariate analysis see: E. R. Malinowski and D. G. Howery, 'Factor Analysis in Chemistry', Wiley–Interscience, New York, 1980. See also: 'Chemometrics: Theory and Application', *ACS Symposium Series No. 52,* B. R. Kowalski, Ed., Am. Chem. Soc., Washington, D.C., 1977.
19 E. R. Malinowski, *Anal. Chem., 49,* 606, 612 (1977).
20 O. Exner, *Collect. Czech. Chem. Commun., 31,* 3222 (1966).
21 a) W. H. Lawton and E. A. Sylvestre, *Technometrics, 13,* 617 (1971). b) E. A. Sylvestre, W. H. Lawton and M. S. Maggio, *ibid., 16,* 353 (1973).
22 a) Z. Z. Hugus, Jr. and A. A. El-Awady, *J. Phys. Chem., 75,* 2954 (1971). b) J. T. Bulmer and H. F. Shurvell, *ibid., 77,* 256, 2085 (1973).
23 This was carried out with the *One Sample Analysis* algorithm of Tektronix PLOT 50 *Statistics Vol. 1* software package.
24 a) C. Daniel and F. S. Wood, 'Fitting Equations to Data', Wiley–Interscience, New York, 1971. b) N. R. Draper and H. Smith, 'Applied Regression Analysis', Wiley, New York, 1966.
25 W. C. Hamilton, 'Statistics in Physical Science', Ronald Press, New York, 1964.
26 W. E. Wentworth, W. Hirsch and E. Chen, *J. Phys. Chem., 71,* 218 (1967).
27 D. W. Marquardt, *JSIAM, 2,* 431 (1963); T. Tabata and R. Ito, *Computer J., 18,* 250 (1975).
28 Tektronix PLOT 50 *Statistics vol. IV* software package.
29 D. M. Olsson and L. S. Nelson, *Technometrics, 17,* 45 (1975).
30 C. A. Brignoli and H. DeVoe, *J. Phys. Chem., 82,* 2570 (1978).
31 a) P. Uguagliati, R. Michelin, U. Belluco and R. Ros, *J. Organometal. Chem., 169,* 115 (1979), and references therein. b) R. R. Krug, W. G. Hunter and R. A. Grieger, *J. Phys. Chem., 80,* 2335 (1976).
32 a) P. J. Lingane and Z. Z. Hugus, Jr., *Inorg. Chem., 9,* 757 (1970). b) T. O. Maier and R. S. Drago, *ibid., 11,* 1861 (1972).